Effect of carbon nanotube surface modification on dispersion and structural properties of electrospun fibers

Xiao-Meng Sui,[1] Silvia Giordani,[2] Maurizio Prato,[2] and H. Daniel Wagner[1,a)]
[1]*Department of Materials and Interfaces, Weizmann Institute of Science, Rehovot 76100, Israel*
[2]*Dipartimento di Scienze Farmaceutiche, INSTM, Unit of Trieste, Piazzale Europa 1, Trieste 34127, Italy*

(Received 4 July 2009; accepted 14 November 2009; published online 9 December 2009)

Covalent surface modification of multiwall carbon nanotubes leads to enhanced nanotube dispersion in the polymer. Despite this, the mechanical properties of electrospun fibers made of polymethylmethacrylate containing surface modified nanotubes generally fall below those of fibers with pristine nanotubes, sometimes below those of pure polymer fibers. We show that covalent functionalization produces defects in the graphene structure, leading to mechanical weakening of the nanotube and, therefore, of the nanocomposite. © *2009 American Institute of Physics*.
[doi:10.1063/1.3272012]

Due to their unique structure, carbon nanotubes (CNTs) are considered, for some time now, as a potentially ideal filler phase to improve the electrical and mechanical properties of polymers.[1–3] This potential however has only partially been realized, especially regarding the mechanical properties, because of a number of potentially detrimental practical obstacles. First, single-wall CNTs (SWCNTs) tend to assemble into aligned bundles because of intertube van der Waals attraction, and multiwall CNTs (MWCNTs) often entangle into more randomly structured packets or "blobs." Second, sp^2 hybridization of carbon atoms[4] and the smooth CNT surface prevent efficient stress transfer from the externally applied load to the reinforcement material, via the polymer matrix. Third, nanotube reinforcement is effective and optimized, only if CNTs can be aligned in the matrix with respect to applied stresses. Such self-attraction and dispersion problems are the main reason behind the contradictory data seen in the literature.

The rapid stretching of fluid jet during electrospinning generates high shear between the polymer chains and the embedded CNTs, leading to CNT alignment and, to some extent, to (polymer) molecular alignment. Polymer chain and CNT alignment are restricted from relaxing back to equilibrium through rapid solvent evaporation, causing the electrospun fiber to solidify immediately.[5–7] Effectively, both the CNTs and the surrounding polymer molecules are spatially confined in a submicron aligned fiber.[8,9]

We recently discovered that the mechanical properties of polymethylmethacrylate (PMMA) electrospun composites based on pristine SWCNTs and MWCNTs were much higher than those of pure PMMA electrospun fibers.[10] In the present paper, we limit ourselves to MWCNT reinforcement and compare the mechanical properties of electrospun PMMA fibers reinforced by two types of surface-modified covalently functionalized MWCNTs, with PMMA fibers reinforced by pristine MWCNTs. Covalent functionalization, which adds functional groups, such as –COOH, to the CNT sidewall, seems to be a promising avenue as it increases both CNT dispersion and stress transfer.[11,12] However, as shown here, if CNT dispersion is indeed finer, covalent functionalization may also negatively affect the structure, resulting in inferior CNT and nanocomposite properties.

We used PMMA (Aldrich) with a molecular weight of ~350 000 g/mol, and pristine and carboxylated MWCNTs (Nanolab). Pristine and carboxylated tubes are termed p-MWCNTs and COOH-MWCNTs, respectively. A second type of MWCNT (Nanocyl-7000) was chemically modified through a 1,3-dipolar cycloaddition reaction of azomethine ylides.[13] This functionalized MWCNT is termed f-MWCNT. We used the same MWCNTs to PMMA weight ratio (1.5%) in all initial composite dispersions, as in our previous work,[10] as it was found to yield a low amount of agglomerates. Dimethylformamide (J. T. Baker) was used as solvent. The electrospinning process and the tensile testing procedure were similar to our earlier work.[10] The testing velocity, 80 μm/min, was the smallest available with the nanomanipulator and was chosen to maintain the test in a quasistatic mode, as needed for proper observation of the fiber local deformation and fracture. The average diameters of the electrospun PMMA, PMMA/p-MWCNTs, PMMA/COOH-MWCNTs, and PMMA/f-MWCNTs fibers were 540 ± 240, 750 ± 260, 750 ± 120, and 690 ± 100 nm, respectively. Slightly finer fibers were used for transmission electron microscope imaging (TEM) (Philips CM-120, 120 kV). Raman CNT spectra were obtained with a Renishaw Ramascope in the backscattering geometry with the 632.8 nm line of a 2 mW HeNe laser. To minimize laser damage, 10% laser intensity was used, and the Raman spectra were collected immediately after focusing. Laser spot was ~5 μm in diameter. Generally, the surface of the CNT reinforced fibers was rougher than that of pure PMMA fibers. Also, as before,[10] the electrospinning process clearly induced CNT orientation.[7,9] We also noticed occasional MWCNT agglomerates and protrusions in some fiber portions, resulting in abrupt lengthwise irregularities and local diameter variability, as observed elsewhere.[8,9] Significantly, these occasional aggregates of functionalized MWCNTs were generally smaller in sizes and less compact than those showing up in pristine MWCNT based fibers, reflecting the improved dispersion of the functionalized MWCNTs compared to pristine MWCNTs. Only fiber specimens without aggregates were tested here.

The experimental results (Table I) reveal that (i) nonfunctionalized (pristine) MWCNT-based PMMA fibers are

a)Electronic mail: daniel.wagner@weizmann.ac.il.

TABLE I. Tensile test data and theoretical predictions for all types of electrospun fibers tested in this study.

Sample type [N][a]	Strain to failure ε_{max} (%)	Strength σ_f (MPa)	Young's modulus E (GPa)	Theoretical Young's modulus (Halpin–Tsai)[b] E (GPa)	Energy absorption G_c (MJ/m^3)
PMMA [17]	23.0 ± 7.7	75.0 ± 10.1	0.82 ± 0.09	—	12.6 ± 5.0
p-MWCNT/PMMA [20]	80.6 ± 30.3	193.8 ± 44.5	2.59 ± 0.56	2.89	133.1 ± 54.1
COOH-MWCNT/PMMA [8]	43.3 ± 15.2	78.3 ± 14.2	1.06 ± 0.21	2.45	32.6 ± 15.0
f-MWCNT/PMMA [8]	16.5 ± 7.3	59.0 ± 12.7	0.94 ± 0.10	2.60	8.7 ± 2.2

[a]N=number of tested specimens.
[b]In the theoretical calculation of Young's modulus all CNT types have an assumed Young's modulus of 450 GPa. The CNT aspect ratio, however, was experimentally measured by using extensive collages of TEM images, yielding values of 180, 110, and 130 for p-MWCNT, COOH-MWCNT, and f-MWCNT, respectively, which result in the slightly different predictions for each nanocomposite type listed in the Table.

considerably stiffer, stronger, and tougher than the fibers based on functionalized MWCNTs, and than pure PMMA fibers; (ii) COOH-MWCNT/PMMA fibers perform better that pure PMMA fibers; and (iii) f-MWCNT/PMMA fibers are mechanically worse than even pure PMMA fibers. The predicted Young's modulus (calculated by the classic Halpin–Tsai model,[8] using equal modulus values for all three CNT types) is significantly larger than the experimental modulus for both types of functionalized CNT based nanocomposites, but quite close to the experimental value for the pristine CNT based nanocomposite. This seems to indicate that functionalized CNTs are structurally affected by the surface chemical treatment, causing a reduction in mechanical performance. Since all fibers had a relatively large diameter (above 650 nm), no observed[14] increase in modulus with decreasing diameter (below about 500 nm) is observed. Typical stress-strain curves (not shown) reveal that the yield point increases to 13.0% for p-CNTs based composite fiber (compared with 8.4% for PMMA fibers), but slightly decreases to 7.6% for f-CNTs based fibers. The elongation of p-MWCNT/PMMA fibers is about three times that of PMMA fiber, due to extensive necking.[10] The relative trend of the experimental "tensile toughness" $G_c = \int \sigma d\varepsilon$, where σ is the tensile stress and ε the strain, is similar to that of the experimental Young's modulus. Thus, despite the improved dispersion of the functionalized CNTs in the polymer, no enhancement in mechanical properties is observed relative to the pristine MWCNT based composite. To explain the lack of mechanical properties enhancement following surface functionalization, we consider the chemistry of the process. Functionalization adds chemical groups to the outermost CNT layer, forming covalent bonds with the carbon atoms. This likely involves introducing sp^3 hybridized carbon atoms to the graphene plane by sacrificing the sp^2 hybridized carbon.[15] In a study of the effect of surface hydrogenization on graphite and CNTs, Volpe and Cleri[16] claim that the C–H bond gives rise to a local tetragonal distortion: the H atom pulls the C atom out of the basal plane. Atomistic simulations indicates that the effect of carbonization has essentially the same effect as hydrogenization,[17] and sp^3 carbon atoms can be seen as defects. Simulations also show that chemical functionalization degrades the mechanical properties of SWCNTs, such as strength, ductility and modulus.[17–19] The preparation of the f-MWCNTs used here involves chemical reaction steps[13] which likely induces even more defects in the CNT structure.

To demonstrate the presence of defects in the functionalized MWCNTs, Raman and TEM characterization were performed. The Raman D band (D=disorder) located at 1320 cm^{-1} (Fig. 1) originates from amorphous carbon and structural defects; the G band (G=graphite) at 1570 cm^{-1} is related to graphite structures, and stems from tangential shearing mode of the carbon atoms.[20–22] The G′ band at 2640 cm^{-1} is an overtone of the D band. The ratio of integrated intensities of the D and G bands, I_D/I_G, can be used to estimate the density of defects in the CNT structure: the larger the value of the I_D/I_G ratio, the higher the defect density.[23,24] As indicated in Fig. 1, the values of I_D/I_G for the functionalized MWCNTs are larger than for pristine MWCNTs, the largest ratio being observed for f-MWCNTs. The same trend is observed by using the ratio of intensities of the D and G′ bands, $I_D/I_{G'}$. Thus, chemical surface modification indeed breeds defects in the CNT structure.

Unlike the smooth and uniform surface of p-MWCNTs, the surfaces of both types of functionalized MWCNTs are rough and uneven, as shown by TEM in Figs. 2(a)–2(c). High resolution micrographs reveal a large density of defects in the outermost layer, including wall irregularities, twisting, and collapse (see arrows). This is especially evident for f-MWCNTs [Fig. 2(c)]. Figures 2(d)–2(f) show the fracture surfaces of the three types of nanofibers tested here. Careful observations reveal significant differences in the interfacial interaction between the polymer matrix and the nanotubes in these three systems. Whereas extensive tube-PMMA pull out is evident in p-MWCNT/PMMA, with clean protruding CNT surfaces being clearly visible [Fig. 2(d)] indicating a weak

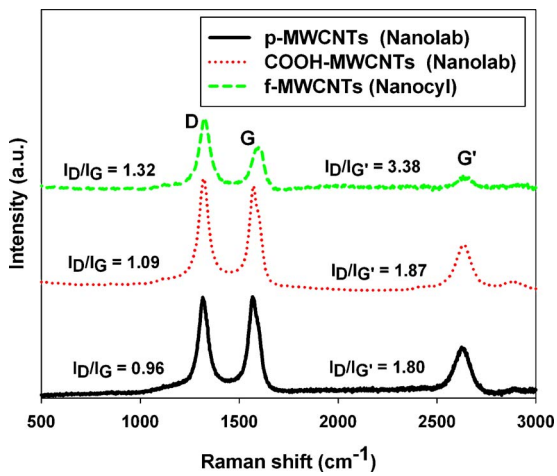

FIG. 1. (Color online) Raman spectra of pristine and functionalized MWCNTs. The ratio I_D/I_G of integrated intensities of the D and G peaks reflects the amount of defects in the CNT structure, with larger ratio values corresponding to higher defect densities (Refs. 23 and 24).

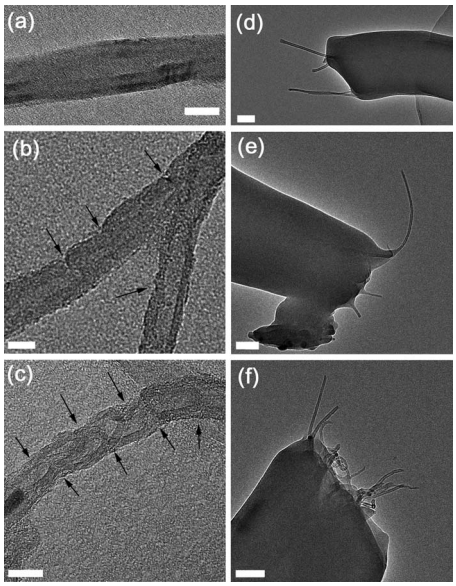

FIG. 2. High resolution TEM images showing (a) quasiperfect microstructure of pristine MWCNTs; [(b) and (c)] defects and structural distortion in functionalized MWCNTs (arrows); CNT pull-out from fracture surfaces of: (d) p-MWCNT/PMMA electrospun fibers; (e) COOH-MWCNT/PMMA; (f) f-MWCNT/PMMA. Scale bars are 10 nm in (a)–(c) and 100 nm in (d)–(f).

interfacial bond, both types of functionalized CNTs are more heavily covered with PMMA, indicating stronger polymer-CNT interactions, and thus improved adhesion and stress transfer. This does not automatically imply that the mechanical properties of the nanocomposites are improved, as indeed seen here: depending on the amount of damage caused to the molecular structure of the CNT surface walls by chemical functionalization, the resulting dissipation of fracture energy, as well as stiffness and strength of the nanocomposites, may either be improved[25] or unaffected by the inclusion of functionalized CNTs. We conclude that surface functionalization of MWCNTs may be viewed as a double-edge sword, which at the same time brings about improved tube dispersion in the polymer mass but also degrades the structural integrity of the tube walls, the consequence of which is a decrease in mechanical properties.

We acknowledge support from the NOESIS European project on "Aerospace Nanotube Hybrid Composite Structures with Sensing and Actuating Capabilities," the G. M. J. Schmidt Minerva Centre of Supramolecular Architectures, the "NES" MAGNET Program of the Israeli Ministry of Industry and Trade, and the University of Trieste, and MIUR (Grant Nos. PRIN 2006, Prot. 2006034372, and FIRB Prot. RBIN04HC3S). The electron microscopy studies were conducted at the Irving and Cherna Moskowitz Center for Nano and Bio-Nano Imaging at the Weizmann Institute of Science. This research was made possible in part by the generosity of the Harold Perlman family. H.D.W. is the recipient of the Livio Norzi Professorial Chair.

[1]R. Haggenmueller, H. H. Gommans, A. G. Rinzler, J. E. Fischer, and K. I. Winey, Chem. Phys. Lett. **330**, 219 (2000).
[2]R. Andrews, D. Jacques, A. M. Rao, T. Rantell, F. Derbyshire, Y. Chen, J. Chen, and R. C. Haddon, Appl. Phys. Lett. **75**, 1329 (1999).
[3]P. M. Ajayan, O. Stephan, C. Colliex, and D. Trauth, Science **265**, 1212 (1994).
[4]P. J. F. Harris, *Carbon Nanotubes and Related Structures* (Cambridge University Press, Cambridge, 1999).
[5]W. Salalha, Y. Dror, R. L. Khalfin, Y. Cohen, A. L. Yarin, and E. Zussman, Langmuir **20**, 9852 (2004).
[6]D. Li and Y. N. Xia, Adv. Mater. **16**, 1151 (2004).
[7]M. Bashouti, W. Salalha, M. Brumer, E. Zussman, and E. Lifshitz, ChemPhysChem **7**, 102 (2006).
[8]L. Q. Liu, D. Tasis, M. Prato, and H. D. Wagner, Adv. Mater. **19**, 1228 (2007).
[9]Y. Dror, W. Salalha, R. L. Khalfin, Y. Cohen, A. L. Yarin, and E. Zussman, Langmuir **19**, 7012 (2003).
[10]X. M. Sui and H. D. Wagner, Nano Lett. **9**, 1423 (2009).
[11]J. N. Coleman, U. Khan, and Y. K. Gun'ko, Adv. Mater. **18**, 689 (2006).
[12]K. Balasubramanian and M. Burghard, Small **1**, 180 (2005).
[13]V. Georgakilas, K. Kordatos, M. Prato, D. M. Guldi, M. Holzinger, and A. Hirsch, J. Am. Chem. Soc. **124**, 760 (2002).
[14]A. Arinstein, M. Burman, O. Gendelman, and E. Zussman, Nat. Nanotechnol. **2**, 59 (2007).
[15]J. L. Bahr and J. M. Tour, J. Mater. Chem. **12**, 1952 (2002).
[16]M. Volpe and F. Cleri, Surf. Sci. **544**, 24 (2003).
[17]Z. Q. Zhang, B. Liu, Y. L. Chen, H. Jiang, K. C. Hwang, and Y. Huang, Nanotechnology **19**, 395702 (2008).
[18]A. Garg and S. B. Sinnott, Chem. Phys. Lett. **295**, 273 (1998).
[19]Y. D. Kuang and X. Q. He, Compos. Sci. Technol. **69**, 169 (2009).
[20]O. Lourie and H. D. Wagner, J. Mater. Res. **13**, 2418 (1998).
[21]A. M. Rao, A. Jorio, M. A. Pimenta, M. S. S. Dantas, R. Saito, G. Dresselhaus, and M. S. Dresselhaus, Phys. Rev. Lett. **84**, 1820 (2000).
[22]A. Jorio, G. Dresselhaus, M. S. Dresselhaus, M. Souza, M. S. S. Dantas, M. A. Pimenta, A. M. Rao, R. Saito, C. Liu, and H. M. Cheng, Phys. Rev. Lett. **85**, 2617 (2000).
[23]A. Swan, in *Measurement Issues in Single Wall Carbon Nanotubes*, edited by S. Freiman, S. Hooker, K. Migler and S. Arepalli (U.S. Government Printing Office, Washington, 2008), p. 43.
[24]N. Lachman, C. Bartholome, P. Miaudet, M. Maugey, P. Poulin, and H. D. Wagner, J. Phys. Chem. C **113**, 4751 (2009).
[25]T. Ramanathan, A. A. Abdala, S. Stankovich, D. A. Dikin, M. Herrera-Alonso, R. D. Piner, D. H. Adamson, H. C. Schniepp, X. Chen, R. S. Ruoff, S. T. Nguyen, I. A. Aksay, R. K. Prud'homme, and L. C. Brinson, Nat. Nanotechnol. **3**, 327 (2008).